A Precise Ranging with Subcarrier Diversity for 5G NR Indoor Positioning

Zhaoliang Liu[1,2], Liang Chen*[1,2], Xin Zhou[2], Yanlin Ruan[2], Zhenhang Jiao[2], Ruizhi Chen[2]

1. Hubei Luojia Laboratory, Wuhan University, Wuhan, China

2. State Key Laboratory of Information Engineering in Surveying, Mapping and Remote Sensing, Wuhan University, Wuhan, China

l.chen@whu.edu.cn

Commission III, WG III/1

KEY WORDS: 5G, Location-based service, Indoor positioning, Ranging, Path loss model.

ABSTRACT:

Indoor positioning is an important component of location-based service. Moreover, it has extensive applications in areas such as the Internet of Things (IoT) and Artificial Intelligence (AI). As a new generation of the mobile communication signal, the introduction of technologies such as multi-carrier, massive multiple-input multiple-output (MIMO), and ultra-dense network (UDN) has enabled 5G NR signal to demonstrate unique technical advantages in the field of indoor positioning. In this paper, for indoor positioning, a subcarrier diversity precision ranging method based on a commercial 5G NR signal is proposed. According to the results of field experiments in the indoor environment, the proposed method significantly improves the ranging precision compared to the Reference Signal Receiving Power (RSRP)-based ranging method. When the diversity ratio is set to 0.25, the 95% cumulative distribution function (CDF) of the overall ranging error is less than 3 meters.

1. INTRODUCTION

High precise Location-Based Service (LBS) is an essential part of the Internet of Things (IoT) and Artificial Intelligence (AI) technologies. As the most widely used and stable positioning system, the Global Navigation Satellite System (GNSS) has always been an important part of LBS. With the development of IoT and AI technology, GNSS is no longer able to meet the demand of high precise LBS in IoT and AI. Indoor positioning technology enables high precise LBS in areas where GNSS is unavailable (e.g. indoors, cities and canyons) by using signals of opportunity (SoP) and multi-source sensor information.

In the research process of indoor positioning technology, the application of WiFi (Zafari et al., 2019), Bluetooth (Chen et al., 2019), and other SoP (Zhou et al., 2020; Chen et al., 2017) has always been the hotspot. Currently, the main indoor positioning technology based on SoP includes fingerprint positioning and geometric intersection positioning. The fingerprint positioning technology usually requires a lot of manpower to build and update fingerprint databases, which makes it difficult to use on a large scale. Geometric intersection positioning technology is limited by the number of indoor base stations (BSs), making it difficult to provide location services on its own. But high precise geometric measurement information is still an important reference for indoor positioning technology. With the continuous improvement of people's demand for location service accuracy and applicability, indoor positioning technology based on the geometric intersection is receiving more attention.

The 5G NR signal is the latest generation of mobile cellular network signals. Since 2018, the 5G network has started to be commercially available worldwide. By the end of 2020, the global 5G network users had reached 220 million (Ericsson Mobility Report, 2020). Compared with previous generations of mobile cellular network signals, the introduction of ultra-dense network (UDN) technology not only increases the density of BS distribution in the outdoor environment but also deploys a large number of BSs in the indoor environment. These BSs provide a large number of available line-of-sight (LOS) signals for the construction of indoor positioning systems (Chen et al., 2021;

Shamaei and Kassas, 2021). Through reasonable use of these LOS signals, high precise indoor positioning systems can be implemented using geometric intersection positioning technology.

High precision ranging is an essential part of geometric intersection positioning technology. The path loss model (PLM) is widely used in wireless ranging because of its simple principle and low complexity. At present, the application of PLM in positioning is relatively straightforward, simply ranging through parameters such as received signal strength (RSS) (Xu et al., 2014) or reference signal receiving power (RSRP) (Çelik et al., 2017) of the signal. These methods do not consider the effect of the complex indoor environment on the power attenuation of different subcarriers. Taking into account the imminent large-scale deployment of 5G networks in the indoor environment and the characteristics of multi-carrier transmission of 5G signals. This paper proposes a subcarrier diversity precision ranging method based on the 5G NR signal according to the signal transmission power variation on different beams and subcarriers caused by the indoor environment. The specific contributions of this paper are as follows:

• This paper considers the multi-beam and multi-carrier characteristics of the 5G NR downlink signal and constructs a subcarrier diversity precision ranging method.

• Through field experiments, the commercial 5G NR downlink signal is used to achieve high precision ranging in the indoor environment.

The rest of this paper is organized as follows: Section II is the system model. Section III is the main setup of the field experiments in the indoor environment. Section IV is the experimental findings. Finally, Section V concludes the paper and indicates future work.

2. SYSTEM MODEL

In the indoor environment, using RSS and RSRP directly as the judgment basis of signal receiving power for ranging will cause a larger measurement error. Based on the PLM, this paper fully considers the multi-beam and multi-carrier characteristics of the
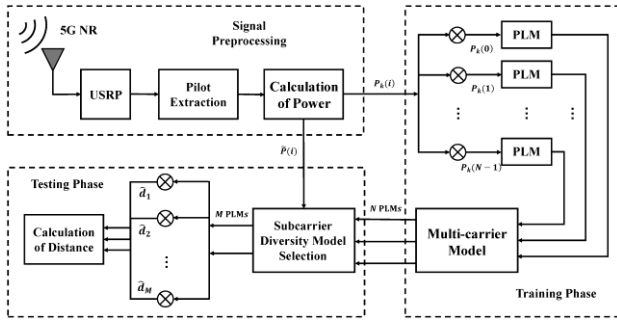
Figure 1. The Flowchart of Subcarrier Diversity Precision Ranging Method.

5G NR downlink signal. A subcarrier diversity precision ranging method based on the 5G NR downlink signal applicable in the indoor environment is proposed. In the training phase, the subcarrier power of different pilots is used to construct PLM respectively. In the test phase, the PLM and power corresponding to some sub-carriers are selected from all sub-carriers through RSRP for precise ranging. The flowchart of the method is shown in Figure 1 and the details are as follows.

2.1 Calculation of Power

In the 5G NR network, the introduction of multi-beam technology will result in different degrees of impact on beam signal propagating from different directions in the indoor environment. There will be LOS and non-line-of-sight (NLOS) signals from different beams anywhere, as well as the multipath component of these LOS/NLOS signals. The power of the signal is also subject to varying degrees of attenuation and superimposition. To measure the signal receiving power more objectively, fully considering the influence of different beams on the environment, according to (1), the combined power of multiple beams on different subcarriers is obtained:

$$P(i) = \frac{1}{N_b} \sum_{j=1}^{N_b} P(i,j) \qquad (1)$$

where N_b is the number of beams, $P(i,j)$ is the power value extracted by the signal receiver on the ith subcarrier of the jth beam, and $P(i)$ is the calculated multi-beam joint power value on the ith subcarrier.

2.2 Multi-carrier PLM

The radio signal is transmitted at the signal transmitter after a gain G_T and is received by the signal receiver after a gain G_R. Theoretically, the amplitude of the power of the received signal decays rapidly as the distance between the signal transmitter and receiver increases. The amplitude P_r of the power of the received signal can therefore be modeled as follows:

$$P_r \propto \frac{G_t \cdot G_r}{4\pi d^n} \cdot P_t \qquad (2)$$

where d is the distance between the signal receiving end and the transmitting end, n is the pass-loss exponent in the current context. The relationship of the signal receiving power and distance can be modelled as a PLM and expressed as follows (Dorf et al., 1997):

$$P_k = P_0 - 10 \cdot n \cdot \log_{10} \frac{d_k}{d_0} + \omega \qquad (3)$$

(a) Test point I (b) Test point II
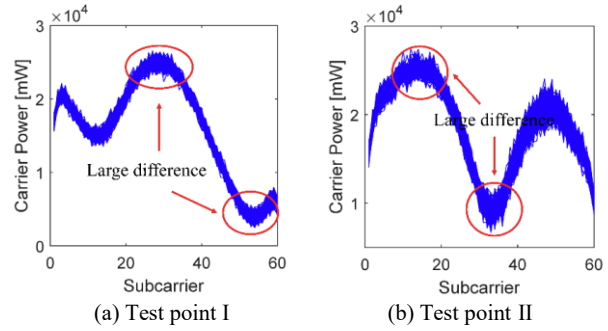
Figure 2. Signal Power on Different Subcarriers.

where P_k is the signal receiving power at k different locations, d_0 is the empirically selected distance between the reference point and the signal transmitter, in this case, we set $d_0 = 1$ m. d_k is the distance between the signal transmitter and the signal receiver, P_0 is a constant, representing the power amplitude of the received signal at the reference point. ω represents Gaussian random noise with zero mean (Mazuelas et al., 2009).

To derive the simple formula between d_k and P_k, it is necessary to assume that P_0 and the pass-loss exponent n remains stable for a short period in a fixed environment [12]. According to the maximum likelihood estimation (MLE), the estimated distance $\hat{d}_k$ between the signal transmitter and the signal receiver can be obtained (Li, 2006):

$$\hat{d}_k = 10^{\frac{P_0 - P_k}{10 \cdot n}} \qquad (4)$$

The transmission status of multi-carrier signals on different subcarriers is different. To accurately express the variation of signal power transmission on different subcarriers, PLMs are built for different subcarriers. The multi-beam joint power $P_k(i)$ at k different locations are substituted into the (3), respectively.

We can obtain the reference point power $P_0(i)$ and pass-loss exponent $n(i)$ of the ith subcarrier. According to the structural characteristics of the Synchronization Signal Block (SSB) of the 5G NR downlink signal, N ($N = 60$) different PLMs can be obtained from the Demodulation Reference Signal (DMRS) on different subcarriers.

2.3 Subcarrier Diversity Model Selection

In the actual ranging process, the signals carried on different subcarriers are affected by the environment differently. It can be seen from Figure 2 that in the 5G signal transmission process, the signal power on different subcarriers varies a lot. According to the multi-beam average power $P(i)$ on different subcarriers, we add a subcarrier diversity process to select a part of the subcarriers to establish diversity ranging.

In the process of subcarrier diversity ranging, the RSRP of the 5G NR downlink signal is used as the basic standard for diversity. We can calculate the RSRP of the received signal based on the DMRS in the 5G NR downlink signal. A set containing M ($M = N \cdot \psi$) pairs of real-time multi-beam joint power $\tilde{P}(i)$ and RSRP absolute differences is conducted, which can be expressed as follows:

$$\{L_1(\tilde{P}(1), \tilde{P}(r)), \dots, L_M(\tilde{P}(M), \tilde{P}(r))\} \qquad (5)$$
$$= \min_{1 \leq i \leq N} L(\tilde{P}(i), \tilde{P}(r))$$

where $\tilde{P}(i)$ is the real-time multi-beam joint power on the ith subcarrier, $\tilde{P}(r)$ is the real-time RSRP of the received signal based on the DMRS in the 5G NR downlink signal. The empirical value ψ is the scale factor to determine the size of the diversity.
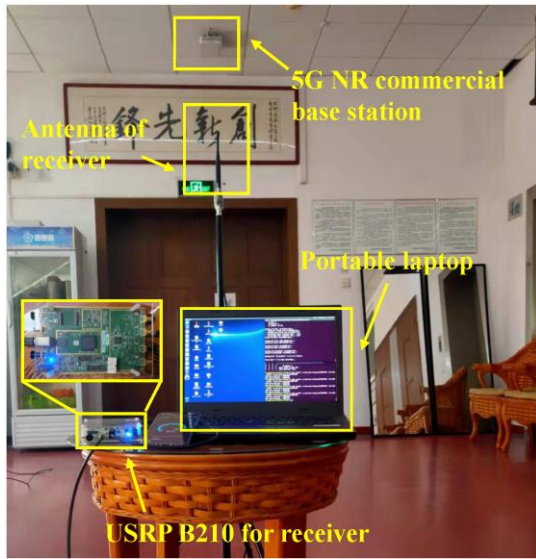
Figure 3. Testing Scenario.

The distance $\{L_1(\tilde{P}(1), \tilde{P}(r)), \ldots, L_M(\tilde{P}(M), \tilde{P}(r))\}$ and $L\left(\tilde{P}(i), \tilde{P}(r)\right) = \left|\tilde{P}(i) - \tilde{P}(r)\right|$ is a set **L** of M minimum distances $L\left(\tilde{P}(i), \tilde{P}(r)\right)$. We choose the PLM and real-time power corresponding to the subcarriers in set **L** to create a real-time diversity.

2.4 Calculation of Distance

According to the established real-time diversity, the $\tilde{P}(i)$ is substituted into the PLMs respectively. Through M PLMs in real-time diversity, M different distance estimation results $\hat{d}_m$ can be obtained. Bring these M results into (6) and get $\hat{D}$ as the final distance calculation result.

$$\hat{D} = \frac{1}{M}\sum_{m=1}^{M}\hat{d}_m \qquad (6)$$

3. FIELD EXPERIMENTS IN INDOOR ENVIRONMENT

During the field experiments, a signal sampling and recording test platform based on USRP (USRP B210, 2021) was developed. As shown in Figure 3, the experimental platform uses a high rate data transfer cable to connect the USRP B210 to a laptop. The receiving antenna is fixed on a 1.2 m high bracket and connected to the receiving port of the USRP B210 through a cable. The GNU Radio (GNU Radio, 2021) software platform is used for data acquisition and storage. The acquired signal data is processed offline through a software-defined receiver built on the laptop.

In order to verify the feasibility and accuracy of the proposed method in this paper, field experiments were completed in two different scenarios. Field experiment 1 was carried out in a complex typical conference room. There is a commercial 5G NR signal micro BS deployed by a mobile operator in the conference room. Field experiment 2 was carried out in a simple open corridor environment, and the experimental scene also had a commercial 5G NR signal micro BS deployed by a mobile operator. Based on the actual deployment of the 5G NR micro BS by the mobile operator and the actual test results at the experimental site, the collection of the 5G NR downlink signal is completed in two scenarios respectively.
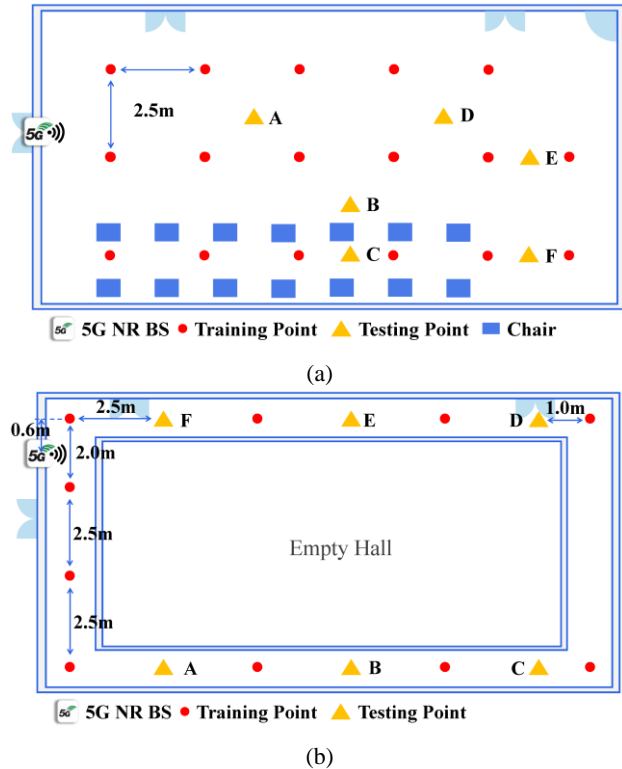
Figure 4. Location of Training and Testing Points. (a) the field experiment 1, (b) the field experiment 2.

Before field experiments, a certain number of training points need to be identified in the experimental environment. In field experiment 1, due to the wide experimental scene, a training point was set every 2.5 m. A total of 17 training points was set at different locations. At the beginning of the experiment, 5G NR downlink signal was collected for 10 s at each training point. This data would be used to train the parameter of the PLM. Afterward, a 5G NR downlink signal was collected at 6 testing points different from the training points for 10 s. These data will be used for the evaluation and analysis of the method. In field experiment 2, due to the narrow experimental scene, a total of 11 different training points was set up in the experimental scene according to the fixed distance interval. At the same time, 5 different representative testing points were selected at the non-training points. And the same method was used to complete the collection of training data and test data. The experimental scenarios and the locations of the training and testing points for the two sets of experiments are shown in Figure 4.

4. RESULTS AND ANALYSIS OF EXPERIMENTS

When the 5G NR downlink signal is received at the receiver, it needs to complete a cell search according to the protocol to obtain synchronization information such as cell ID and signal start location. Based on the results of cell search, coarse synchronization and OFDM demodulation can be completed to obtain the complete 5G NR downlink SSB. The DMRS can then be extracted as the pilot to calculate the different subcarrier power of the received signal based on the synchronization information. The signal power on different subcarriers is the application data of the method constructed in this paper.

4.1 Result Analysis

The proposed method is fully validated and analyzed based on the training data and test data obtained from the two sets of
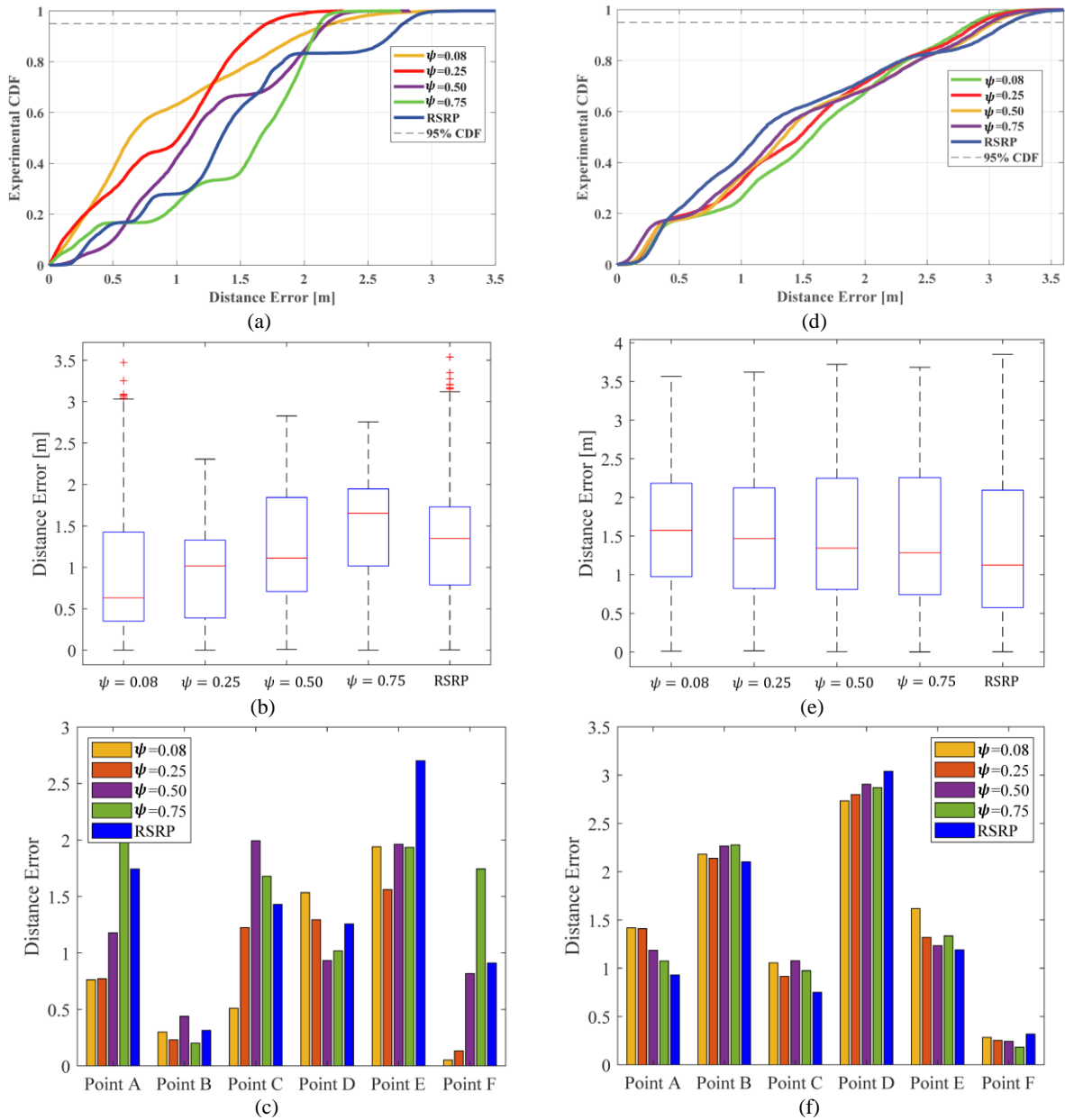
Figure 5. Comparison of Distance Errors in Calculation Results under Different Methods. (a) CDF, (b) boxplot, and (c) grouped bar chart of field experiment 1. (d) CDF, (e) boxplot, and (f) grouped bar chart of field experiment 2.

experiments involved in the paper. Applying this method to an indoor environment can effectively obtain the distance between the receiver and the BS with a commercial 5G NR downlink signal. For the same training data and testing data, we respectively calculated the ranging results of the RSRP-based method and the method proposed in this paper and compared the overall ranging accuracy of the two methods. For the two sets of field experiments in different scenarios, we have made detailed statistics of their accuracy separately. Figure 5 shows the statistical results of the distance error for field experiments. We can clearly see from Figure 5(a) that the distance error is the smallest when $\psi = 0.25$, and its 95% cumulative distribution function (CDF) is 1.73 m. The distance error based on the RSRP method is the largest, and its 95% CDF is 2.80 m. Figure 5(d) shows the statistical results of the distance error of field experiment 2. The results have a high similarity with field experiment 1. The distance error is the smallest when $\psi \in$

(0.08,0.25), and its 95% CDF is less than 3.00 m. The distance error based on the RSRP method is the largest, and its 95% CDF is 3.19 m. It can be seen from the boxplots in Figure 5(b) and Figure 5(e) that when the diversity ratio $\psi = 0.25$, the upper limit of the distance error of the two sets of experimental results relatively low, and there are no obvious abnormal experimental results.

We also made statistics on the mean absolute error of different test points in the two sets of experiments, and compared the error of the method proposed in this paper and the RSRP-based respectively. As shown in Figure 5(c) and Figure 5(f), the abscissa of the bar chart corresponds to different test points, and the ordinate is the distance error of different methods. In field experiment 1, the method proposed in this paper is more stable in complex scenarios and the overall accuracy is higher than that of the RSRP-based method. In field experiment 2, the proposed method in this paper has the same ranging accuracy as the RSRP-

(a) field experiment 1   (b) field experiment 2
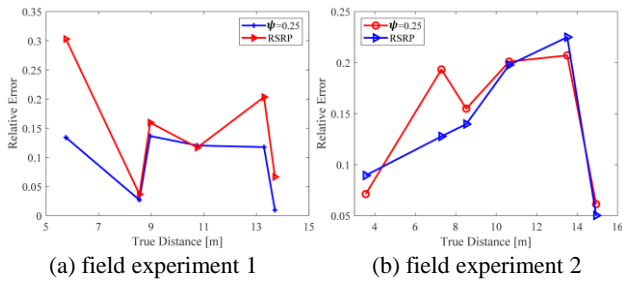
Figure 6. Comparison and Analysis of Actual Distance and Relative Error

Table 1 Result of Overall Error Statistics in Experiments.

Test	Method	RMSE(m)	ME(m)	95% CDF(m)
No.1	$\psi = 0.08$	0.90	3.47	2.25
	$\psi = 0.25$	0.88	2.31	1.73
	$\psi = 0.50$	1.22	2.83	2.19
	$\psi = 0.75$	1.43	2.75	2.13
	RSRP	1.39	3.54	2.80
No.2	$\psi = 0.08$	1.55	3.56	2.89
	$\psi = 0.25$	1.47	3.62	2.95
	$\psi = 0.50$	1.49	3.72	3.06
	$\psi = 0.75$	1.45	3.68	3.03
	RSRP	1.40	3.85	3.19

based method in the simple scenario. In the statistics, we found that there is a large difference in measurement accuracy between the two groups of experiments at different test points, so we further calculated whether there is a difference between the measurement accuracy and the actual measurement distance. As shown in Figure 6, for statistical and observation purposes, only the statistical results of the distance measurement relative error with respect to the actual measured distance for the proposed method in this paper in the case of $\psi = 0.25$ and the RSRP-based method are shown. According to the present results, the overall distance measurement relative error of the two sets of experiments is less than 20%, and there is no obvious change pattern with the increase of the actual measurement distance. Meanwhile, the accuracy based on the method proposed in this paper in field experiment 1 is significantly higher than that based on RSRP.

The root mean square error (RMSE), maximum error (ME), and 95% CDF error statistics for the RSRP-based ranging method and the method proposed in this paper with different diversity ratios are shown in Table 1. It can be seen that the error when using RSRP directly for ranging is significantly higher than the error using the method proposed in this paper. After comparing the results of the two sets of experiments, we can find that the method proposed in this paper has better application in the complex and variable conference room scenes. In the relatively simple and empty open corridor environment, although the proposed method still has high ranging accuracy, the accuracy improvement is not obvious compared with the RSRP-based method. This indicates that the proposed method has higher applicability in the complex indoor environment.

4.2 Method Analysis

In the subcarrier diversity ranging method, the constants P_0 and the pass-loss exponent n selected from several different subcarrier corresponding PLMs according to the rules are the main factors affecting the ranging results. Therefore, we performed a statistical analysis of two key parameters in the PLM
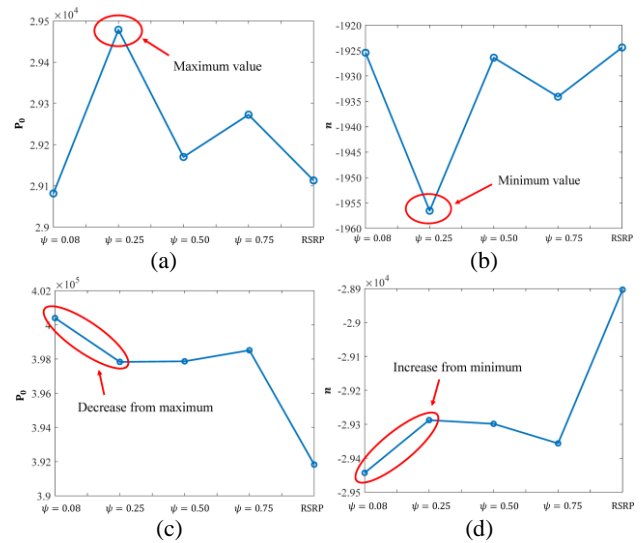
Figure 7. Statistics of Diversity Model Parameters. (a) P_0 and (b) n of field experiment 1. (c) P_0 and (d) n of field experiment 2.

(a) Test point C of field experiment 1

(b) Test point C of field experiment 2
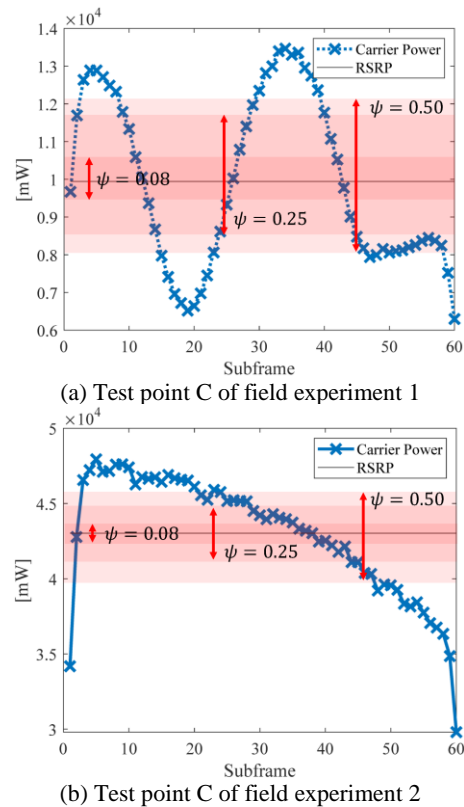
Figure 8. Selected Subcarriers under Different Diversity Ratio.

obtained by the proposed method and the RSRP-based method in Figure 7. In field experiment 1, the maximum range accuracy is achieved with $\psi = 0.25$, when P_0 in PLM has the maximum value and n has the minimum value, according to the known results. In field experiment 2, the range accuracy is relatively high with $\psi \in (0.08, 0.25)$, when P_0 in the PLM is in the variation of decreasing from the maximum value and n is in the variation of increasing from the minimum value. This proves that the accuracy of PLM is closely related to the two parameters P_0 and n. And, in the same scenario, we have reason to believe that ranging with different methods for PLM regression, when the P_0

(a) The Result of Form Factor   (b) The Result of Kurtosis
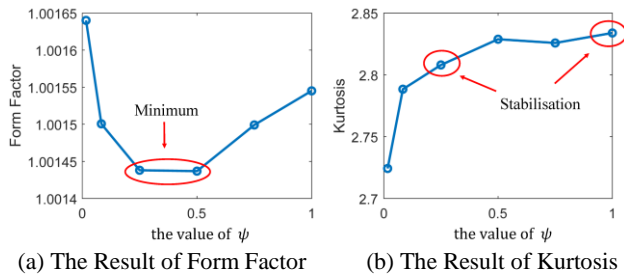
Figure 9. Comparison of Feature for Signal Power in Subcarrier Diversity under Different Diversity Ratio

regression value is relatively large and the n regression value is relatively small, there may be higher ranging accuracy.

Considering the measurement accuracy differences of the method proposed in this paper in different scenarios. And in field experiment 2, the proposed method in this paper did not improve the ranging accuracy much compared to the RSRP-based method. Therefore, we analyzed the test point data in different scenarios from the perspective of data. As shown in Figure 8, the average value of the received signal carrier energy for 10 s continuously at a random test point in field experiment 1 and field experiment 2. In Figure 8(a), the energy fluctuations of different subcarriers are large, which may be caused by refraction and diffraction occurring during signal transmission in complex scenes. The method proposed in this paper achieves relatively good measurement results for signals in such complex scenes with strong energy fluctuations. In Figure 8(b), the energy on the subcarriers on both sides of the channel is low, and the energy on the intermediate subcarriers is high and stable. This phenomenon may be the result of the stronger LOS signal energy and weaker multipath phenomenon in the simple scenario. Compared with the RSRP-based method, the proposed method in this paper does not improve the ranging accuracy significantly for such simple scenes with stable signal energy. Therefore, based on the test data and test results, the proposed method has a stronger potential for application in complex indoor scenes.

At the same time, the known results showed that the overall error at the different test points is relatively stable when $\psi = 0.25$ and that there is no significant distance error, making it suitable as a choice when estimating distances. To explore the intrinsic relationship between the diversity ratio ψ and ranging accuracy, we counted the average value of form factor (Cai et al., 2017) and kurtosis (Zarzoso et al., 2008) of each subcarrier power in the subcarrier diversity under different diversity ratios. Figure 9(a) is the form factor statistics result of the subcarrier power of all test points when the diversity ratio ψ is different. When the diversity ratio $\psi \in (0.25, 0.50)$, the subcarrier power in the real-time diversity has the smallest form factor. At this time, there is no obvious abnormal value in the subcarrier power in the diversity. Figure 9(b) is the kurtosis statistics result of the subcarrier power of all test points when the diversity ratio ψ is different. When the diversity ratio $\psi \geq 0.25$, the kurtosis of the subcarrier power in the real-time diversity tends to be stable, and the subcarrier power of each subcarrier in the diversity is close to a normal distribution. Combined with the form factor and kurtosis, when the diversity ratio $\psi = 0.25$, the subcarrier power in the diversity is normally distributed and there are no obvious outliers. At this time, the PLM and subcarrier power in the subset can be used to obtain more accurate ranging results.

5. CONCLUSION

In this paper, a commercial 5G NR signal is used in the research of indoor positioning technology. A subcarrier diversity precision ranging method for commercial 5G NR signal that can be used in the indoor environment is constructed. In addition, the effectiveness of the method in indoor environmental ranging was verified by field experiments.

According to the results of field experiments, the subcarrier diversity precision ranging method proposed in this paper is feasible. For different test points, the method proposed in this paper can achieve more precise ranging results in the indoor environment. In addition, the ranging results varies according to different diversity ratio ψ. According to the existing experimental results in this paper, the overall precision is highest when $\psi = 0.25$. Also, compared to the RSRP-based ranging method, the method proposed in this paper has higher ranging precision in field experiments. It can prove the effectiveness of the proposed method. In the future, we will make full use of the characteristics of 5G NR UDN technology to build a stable and precise positioning system for indoor positioning.

REFERENCES

Zafari F., Gkelias A., and Leung K. K., 2019. A Survey of Indoor Localization Systems and Technologies. *IEEE Communications Surveys Tutorials*, vol. 21, no. 3, pp. 2568–2599. DOI: 10.1109/COMST.2019.2911558.

Chen L., Kuusniemi H., Chen Y., Liu J., Pei L., Ruotsalainen L., and Chen R., 2015. Constraint Kalman Filter for Indoor Bluetooth Localization. in *2015 23rd European Signal Processing Conference (EUSIPCO)*, pp. 1915–1919. DOI: 10.1109/EUSIPCO.2015.7362717.

Zhou X., Chen L., Yan J., and Chen R., 2020. Accurate DOA Estimation With Adjacent Angle Power Difference for Indoor Localization, *IEEE Access*, vol. 8, pp. 44 702–44 713. DOI: 10.1109/ACCESS.2020.2977371.

Chen L., Yang L.-L., Yan J., and Chen R., 2017. Joint Wireless Positioning and Emitter Identification in DVB-T Single Frequency Networks, *IEEE Transactions on Broadcasting*, vol. 63, no. 3, pp. 577–582. DOI: 10.1109/TBC.2017.2704422.

Ericsson Mobility Report. accessed. [Online]. Available: https://www.ericsson.com/en/press-releases/2020/11/more-than-1-billion-people-will-have- access-to-5g-coverage-by-the-end-of-2020.

Chen L., Zhou X., Chen F., Yang L. -L. and Chen R., 2021. Carrier Phase Ranging for Indoor Positioning with 5G NR Signals," in *IEEE Internet of Things Journal*. DOI: 10.1109/JIOT.2021.3125373.

Shamaei K. and Kassas Z. M., 2021. Receiver Design and Time of Arrival Estimation for Opportunistic Localization with 5G Signals, *IEEE Transactions on Wireless Communications*, pp. 1–1. DOI: 10.1109/TWC.2021.3061985.

Xu Y., Zhou J., and Zhang P., 2014. RSS-based Source Localization when Path-loss Model Parameters are Unknown,

IEEE Communications Letters, vol. 18, no. 6, pp. 1055–1058. DOI: 10.1109/LCOMM.2014.2318031.

Çelik G., Çelebi H., and Tuna G., 2017. A Novel RSRP-based E-CID positioning for LTE networks, in *2017 13th International Wireless Communications and Mobile Computing Conference (IWCMC)*, pp. 1689–1692. DOI: 10.1109/IWCMC.2017.7986538.

Dorf R., Simon M., Milstein L., and Wan Z., 1997. Digital Communications, *McGraw-Hill*. DOI: 10.1109/TASSP.1984.1164265.

Mazuelas S., Bahillo A., Lorenzo R. M., Fernandez P., Lago F. A., Garcia E., Blas J., and Abril E. J., 2009. Robust Indoor Positioning Provided by Real-time RSSI Values in Unmodified Wlan Networks, *IEEE Journal of Selected Topics in Signal Processing*, vol. 3, no. 5, pp. 821–831. DOI: 10.1109/JSTSP.2009.2029191.

Li X., 2006. RSS-based Location Estimation with Unknown Pathloss Model, *IEEE Transactions on Wireless Communications*, vol. 5, no. 12, pp. 3626–3633. DOI: 10.1109/TWC.2006.256985.

Zhuang Y., Yang J., Qi L., Li Y., Cao Y., and El-Sheimy N., 2018. A Pervasive Integration Platform of Low-cost Mems Sensors and Wireless Signals for Indoor Localization, *IEEE Internet of Things Journal*, vol. 5, no. 6, pp. 4616–4631. DOI: 10.1109/JIOT.2017.2785338.

USRP B210. [Online]. Available: https://www.ettus.com/all-products/ub210-kit/

GNU Radio. [Online]. Available: https://www.gnuradio.org/

Cai X., Han K., Wang L., and Ma L., 2017. Unified Sensor Based Classificaiton Model Across form Factors, in *2017 IEEE SENSORS*, pp. 1–3. DOI: 10.1109/ICSENS.2017.8234209.

Zarzoso V., Phlypo R., and Comon P., 2008. A Contrast for Independent Component Analysis with Priors on the Source Kurtosis Signs, *IEEE Signal Processing Letters*, vol. 15, pp. 501–504. DOI: 10.1109/LSP.2008.919845.